



The QCD phase diagram from functional methods

Lisa M. Haas^{1,2}, Jens Braun³ and Jan M. Pawłowski^{1,2}

¹Institut für Theoretische Physik, Universität Heidelberg, Philosophenweg 16, 69120 Heidelberg

²ExtreMe Matter Institute EMMI, GSI, Planckstr. 1, 64291 Darmstadt

³Friedrich-Schiller-Universität Jena, Theoretisch-Physikalisches Institut, Max-Wien Platz 1, 07743 Jena



Introduction

Quantum Chromodynamics (QCD) at non-zero temperature and density is a very active area of research.

One interesting question is the relation between the chiral (χ) phase transition from microscopic degrees of freedom, quarks and gluons, to macroscopic bound states, hadrons and the confinement-deconfinement phase transition from the quark-gluon plasma at high temperature and density to the hadronic phase at low temperature and density.

An understanding of this interrelation in terms of microscopic dofs is complicated by the fact that one needs to bridge the gap between a deconfined chirally symmetric regime and a confined regime with broken chiral symmetry.

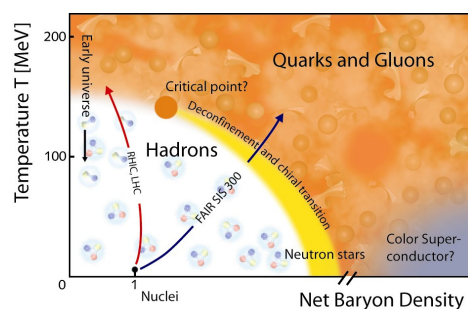


Fig. 1: The phase diagram of QCD. (credits: GSI Darmstadt)

QCD with functional methods

We compute the QCD effective action with functional RG techniques, which allows us to include all quantum fluctuations stepwise at each momentum scale k . This is achieved by integrations over small momentum shells, generating a flow from the microscopic action S_{bare} in the UV towards the macroscopic action Γ in the IR.

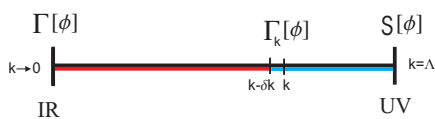


Fig. 2: Momentum modes above k are integrated out, modes below are suppressed due to the regulator.

In our dynamical two-flavour calculation [1] in the chiral limit we include the glue sector of QCD and the matter sector [2] and couple them via dynamic quark gluon interactions. The confining properties are included via the full momentum dependence of the ghost and gluon propagators [3, 4], the matter sector incorporates dynamical mesonic degrees of freedom [2, 5, 6].



Fig. 3: Diagrammatic representation of the flow of the effective action. The cross denotes the regulator function which ensures stepwise integration over small momentum shells.

Imaginary chemical potential

Roberge-Weiss phase transition

At imaginary chemical potential $\mu = 2\pi T i \theta$ the effective action of QCD is periodic: $\text{QCD}_\theta = \text{QCD}_{\theta+\theta_z}$, where $\theta_z = 0, 1/3, 2/3$ for $SU(3)$, as $\theta \rightarrow \theta + \theta_z$ is canceled by the center transformations of the fields. Quantities related to the effective action show the same periodicity (Roberge-Weiss (RW) periodicity), e. g. the chiral condensate $\langle \bar{\psi}\psi \rangle$. QCD_θ is smooth until $\theta = 1/6$ but then shows a discontinuity: the Polyakov loop RW phase transition at T_{RW} .

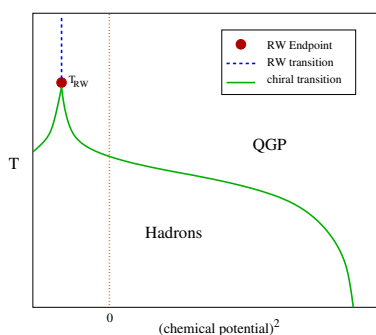


Fig. 4: QCD phase diagram including imaginary chemical potential.

Results at vanishing μ

At vanishing chemical potential we compute the Polyakov loop $L = \frac{1}{N_c} \text{Tr} \mathcal{P} e^{i \int_0^\beta dt A_0}$, the dual density and the pion decay constant and we find close critical temperatures for the deconfinement T_{deconf} and the chiral T_χ transition.

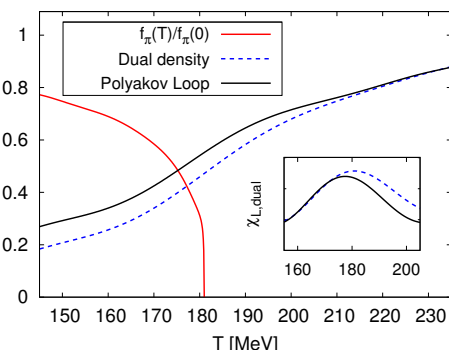


Fig. 5: The pion decay constant, the dual density and the Polyakov loop as functions of temperature, $\chi_L = \partial_\Gamma L[\langle A_0 \rangle]$, $\chi_{\text{dual}} = \partial_\Gamma \bar{n}$.

In [7] so-called dual order parameters have been defined. For dynamical quarks simple functional relations (DSE/FRG) require the extension of the formalism in [7] to imaginary chemical potential, this has been done in [1]. An example of these dual order parameters is the dual density $n_\theta \sim \int \langle \bar{\psi} \gamma_0 \psi \rangle_\theta$. Here, we also compare the critical temperatures for the deconfinement transition given by the Polyakov loop and the dual density. χ_L and χ_{dual} show a peak at the same temperature, which provides a consistency check for our calculation.

Results at imaginary μ

The chiral phase transition

Here we plot the pion decay constant as a function of temperature and imaginary chemical potential. The pion decay constant shows the RW periodicity in θ , it is non-zero below T_χ and vanishes above.

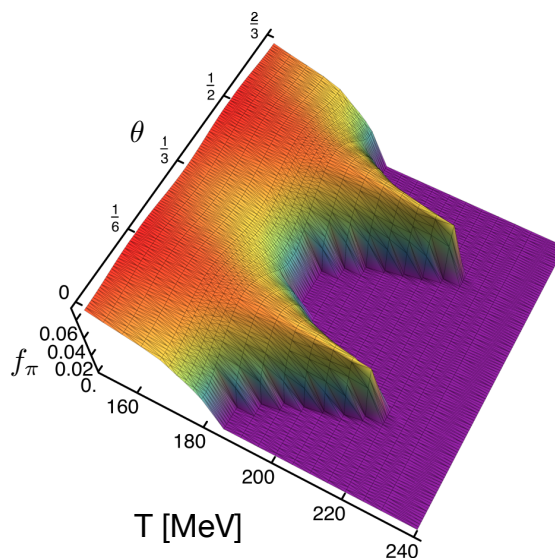


Fig. 6: The pion decay constant as a function of temperature and imaginary chemical potential.

The chiral and deconfinement transition

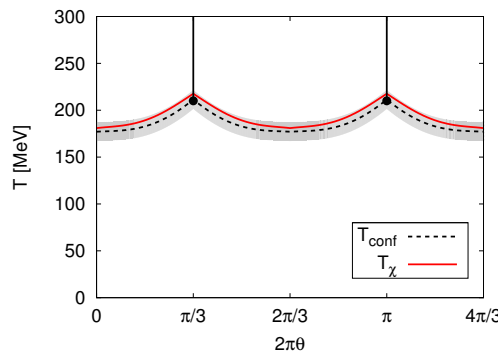


Fig. 7: T_χ and T_{deconf} as functions of temperature and imaginary chemical potential. The shaded area indicates the width of χ_L .

Our results for the phase diagram at imaginary chemical potential show that the chiral and the deconfinement transition agree within the width of χ_L for all θ . We find the predicted RW symmetry. Our result compares qualitatively well with lattice QCD calculations [8]. The parameters of the PNJL model calculations can be adjusted such that their result agrees with lattice calculations [9]. In our calculation the coinciding critical temperatures are solely due to the interplay of quantum fluctuations and are not adjusted by hand.

Polyakov loop potential

The YM Polyakov loop potential shows a phase transition at $T_c = 276$ MeV [3], the QCD glue potential at $T_c = 203$ MeV [10].

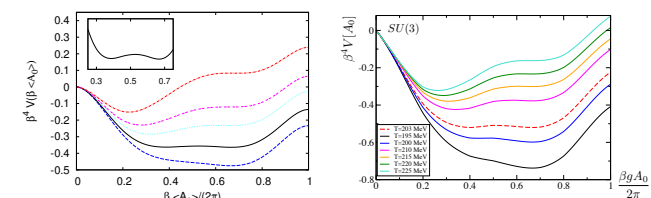


Fig. 8: $SU(3)$ YM potential (left panel) [3] and $SU(3)$ QCD glue potential (right panel) [10] for various temperatures.

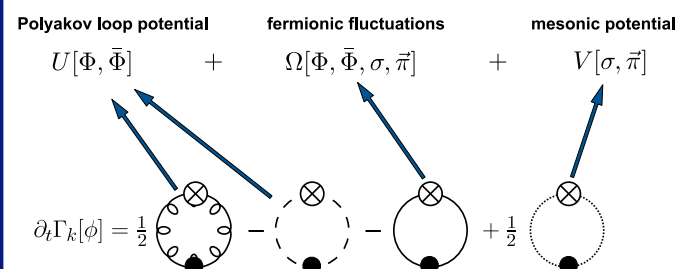


Fig. 9: Comparison of PQM input and FRG QCD output. The FRG provides QCD glue results as input for PQM calculations. $\Phi = \langle L \rangle$ is the expectation value of the Polyakov loop.

PQM calculations use a fit to YM thermodynamics for the Polyakov loop potential. The YM and the QCD glue potential have a similar form but differ in temperature scale.

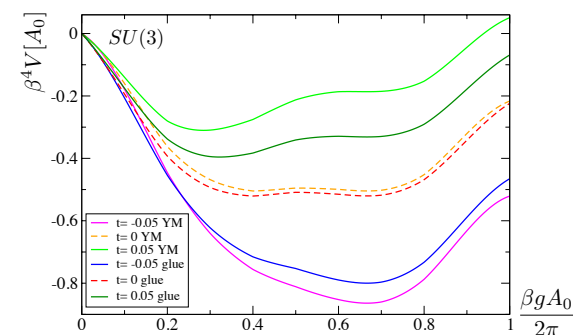


Fig. 10: Comparison of the YM and the QCD glue potential for various reduced temperatures $t = \frac{T}{T_c}$.

The Polyakov loop potentials can therefore be approximately related by

$$(\beta^4 V)_{\text{QCD}}[t, A_0] \simeq (\beta^4 V)_{\text{YM}}[t_{\text{YM}}(t), A_0],$$

which can be used in PQM studies to model QCD glue dynamics. Especially the (reduced) YM temperature is given as a function of the QCD glue temperature $t_{\text{YM}}(t)$.

Outlook

Extend to $N_f = 2+1$ real chemical potential, include better resolution of finite temperature propagators (see talk of L. Fister) and resolve RW endpoint at imaginary chemical potential.

References

- [1] J. Braun, L. M. Haas, F. Marhauser, J. M. Pawłowski, Phys. Rev. Lett. **106**, 2011.
- [2] J. Braun, Eur. Phys. J. C **64**, 2009.
- [3] J. Braun, H. Gies, J. M. Pawłowski, Phys. Lett. B **684**, 2010.
- [4] C. S. Fischer, A. Maas, J. M. Pawłowski, Annals Phys. **324**, 2009; J. M. Pawłowski, in preparation.
- [5] H. Gies, C. Wetterich, Phys. Rev. D **69**, 2004; J. Braun, H. Gies, JHEP **0606**, 2006.
- [6] J. Berges, N. Tetradis, C. Wetterich, Phys. Rept. **363**, 2002; B. J. Schäfer, J. Wambach, Nucl. Phys. A **757**, 2005.
- [7] C. Gatttringer, Phys. Rev. Lett. **97**, 2006; F. Synatschke, A. Wipf, C. Wozar, Phys. Rev. D **75**, 2007; E. Bilgici, F. Bruckmann, C. Gatttringer, C. Hagen, Phys. Rev. D **77**, 2008; E. Bilgici *et al.*, Few Body Syst. **47**, 2010; C. S. Fischer, Phys. Rev. Lett. **103**, 2009.
- [8] S. Kratochvila, P. de Forcrand, Phys. Rev. D **73**, 2006; L. K. Wu, X.-Q. Luo, H.-S. Chen, Phys. Rev. D **76**, 2007.
- [9] Y. Sakai, K. Kashiwa, H. Kouno, M. Yahiro, Phys. Rev. D **77**, 2008.
- [10] J. Braun, L. M. Haas, J. M. Pawłowski, in preparation.